

Electron Injection Efficiency from Excited N3 into Nanocrystalline ZnO Films: Effect of (N3–Zn²⁺) Aggregate Formation

Hiroaki Horiuchi,[†] Ryuzi Katoh,^{*,†} Kohjiro Hara,[†] Masatoshi Yanagida,[†] Shigeo Murata,[†] Hironori Arakawa,[†] and M. Tachiya[‡]

Photoreaction Control Research Center (PCRC), National Institute of Advanced Industrial Science and Technology (AIST), 1-1-1 Higashi, AIST-Tsukuba Central 5, Tsukuba, Ibaraki 305-8565, Japan

Received: September 5, 2002; In Final Form: January 5, 2003

Dye-sensitized solar cells based on *cis*-bis-(4,4'-dicarboxy-2,2'-bipyridine) dithiocyanato ruthenium (II) (Ru(dcbpy)₂(NCS)₂, N3) adsorbed on nanocrystalline ZnO films are a promising system as highly efficient solar cells. However, the performance of the cells decreases with increasing concentration of N3 dye on the surface of ZnO films, suggesting the formation of aggregates. We have studied the efficiency of electron injection at two concentrations through fluorescence and transient absorption measurements. From fluorescence measurements, we confirmed that the aggregates (N3–Zn²⁺) of N3 dyes with Zn²⁺ ions are formed in ZnO films and electron injection from (N3–Zn²⁺) to ZnO films is inefficient. Fluorescence and scanning electron microscope measurements show that the aggregate forms not only in meso pore of ZnO films but also at the surface as micrometer-sized particles. From transient absorption measurements, it is found that the efficiency of the electron injection is decreased by the presence of (N3–Zn²⁺) on the surface of ZnO films.

Introduction

Highly efficient dye-sensitized solar cells based on molecular sensitizers adsorbed on nanocrystalline TiO₂ films were developed,¹ and much effort has been made to improve solar cell performance.² Figure 1 shows the primary steps of the dye-sensitized solar cells. Upon photoexcitation of the sensitizer dyes, the electrons are injected from the excited sensitizer dyes to the conduction band (CB) of the semiconductor film (electron injection). The injected electrons recombine with the oxidized sensitizer dyes (recombination). The recombination process is in competition with the reduction of the oxidized sensitizer dyes by the redox mediator molecules (I[–]/I₃[–]) (regeneration). The remaining electrons can be transported in the semiconductor film as conducting electrons. The conducting electrons can react with the redox mediator molecules during the transport before reaching the back contact electrode (dark current) and, finally, the remainder flow into the external circuit.

To collect incident photons efficiently, the density of sensitizer molecules on the surface has to be high. Under this condition, aggregation of sensitizer molecules often occurs on the surface. One of the most important aggregates for the electron injection process is the J aggregate, in which several planar molecules are stacked in parallel. Formation of J aggregates leads to narrowing and red-shifting of the absorption spectrum.^{3,4} Moreover, electron injection from J aggregates is known to be very efficient.⁵ For this reason, J aggregates of cyanine dyes have been used in the photographic industry.⁵ The H aggregate, in which two molecules are placed in parallel, are often observed in aqueous solutions of organic dyes such as eosin-Y and rhodamine 6G.⁷ Its absorption band is blue-shifted compared to that of the monomer.⁷ In H aggregates of

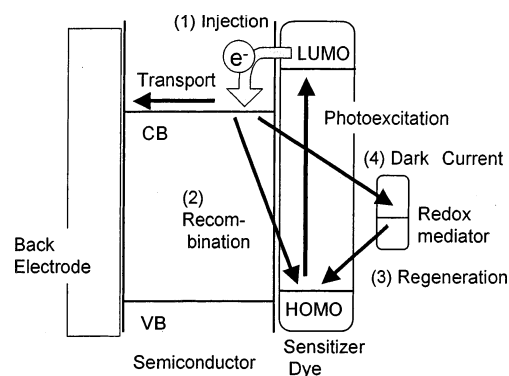


Figure 1. Energy level diagram of the electron injection and other relaxation pathways.

rhodamine 6G in aqueous solution, very rapid relaxation from the singlet excited state to the ground state occurs in 100 ps time range.⁸ This fast relaxation is not due to rapid formation of the triplet state (intersystem crossing) but probably due to efficient internal conversion to the ground state.⁹ This implies that the electron injection efficiency from H aggregates is expected to be small. It should be emphasized that the photochemical properties of molecular aggregates are significantly different from those of monomers.

In dye-sensitized solar cells, it has been often observed that the solar cell performance is lowered by the aggregation of sensitizer dyes. It is known that the performance of some dye-sensitized solar cells are improved by reducing the density of sensitizer dyes on the surface by addition of coadsorbates.¹⁰ When Cresyl Violet, Pinacyanol, and Rhodamine 6G are used as sensitizer molecules, H aggregates are formed on the surface of nanocrystalline semiconductor electrodes. The IPCE (photon-to-current conversion efficiency) of the solar cells is considerably low,¹¹ suggesting that the electron injection is hindered by the formation of H aggregates. On the contrary, solar cell performance is improved by the formation of J aggregates.

* To whom correspondence should be addressed. E-mail: r-katoh@aist.go.jp.

[†] PCRC, AIST.

[‡] AIST.

Sayama et al. reported that the dye-sensitized solar cells with J aggregates of benzothiazole merocyanine on the surface of TiO₂ show high IPCE,¹² suggesting that efficient electron injection occurs from the J aggregates. The absorption spectrum of the J aggregate is red-shifted compared to that of the monomer, and therefore, the light harvesting efficiency is also improved. These facts clearly indicate that the electron injection process is influenced by aggregation of dye molecules. It is important to study the properties of aggregates for the development of high performance solar cells.

Nanocrystalline TiO₂ films are considered to be the most promising material to realize high performance dye-sensitized solar cells. Nanocrystalline ZnO films have also been studied as semiconductor electrodes for the dye-sensitized solar cells.^{13,14,15} To fix sensitizer dyes on ZnO surfaces, ZnO films are immersed into the solution of sensitizer dyes. During the process, a small amount of Zn²⁺ ions are dissolved into the solution from the surface of the ZnO films, and subsequently, aggregation of sensitizer dyes with Zn²⁺ ions occurs. These types of aggregates were reported for several organic sensitizer dyes^{16,17} as well as ruthenium complexes.¹⁸ Concerning the effect of the aggregation on the performance of dye-sensitized solar cells, the IPCE dramatically decreases with increasing immersing time of ZnO substrates in N3 dye solution.¹⁸ This implies that the electron injection efficiency is hindered by the formation of the aggregate (N3–Zn²⁺) between N3 dye and Zn²⁺ ions, although no direct experimental evidence has been reported.

Here we study the excited-state properties of the aggregate (N3–Zn²⁺) by fluorescence and transient absorption spectroscopy. The formation of (N3–Zn²⁺) can be confirmed by the peak position of the fluorescence spectrum. From the fluorescence decay measurement, it is found that the electron injection from excited (N3–Zn²⁺) to ZnO films is inefficient. The reason may be attributable to the formation of micrometer-sized particles of (N3–Zn²⁺) on the surface, which is confirmed by fluorescence and electron microscopy. The effect of the aggregation on the electron injection efficiency can be evaluated by transient absorption measurements.

Experimental Section

ZnO paste composed of ZnO nanoparticles (Sumitomo Osaka Cement, #100), polyvinyl acetal (Sekisui Kasei, BM-2), and α -terpineol were painted on a glass plate with a screen printer (Mitani Electronics Co., MEC-2400). Nanocrystalline films were prepared by calcination of the painted substrate for 1 h at 420 °C. The thickness of the films was about 5 μ m, and the films were optically transparent. The apparent area of the ZnO films was about 1 cm² (1 cm \times 1 cm). The nanocrystalline films were immersed into the N3 solution of dehydrated ethanol and kept at 25 °C to fix the N3 onto the surface of the ZnO. The immersing time was changed to control the amount of adsorbed N3. The sample specimens were rinsed by ethanol just after the adsorption process to remove the dye solution from the surface. The specimens with the immersing times of 3 min and 12 h are hereafter called dil N3/ZnO and conc N3/ZnO, respectively. For the authentic material, the aggregate (N3–Zn²⁺) was synthesized separately by reported procedure¹⁸ and was cast on a glass plate to make a film.

Absorption spectra were measured with an UV–vis spectrophotometer (Shimadzu, UV-3101PC). Fluorescence spectra were measured with a gated-CCD (Roper Scientific, ICCD-MAX) camera after being dispersed with a monochromator (Acton, SpectraPro-308). The second harmonic pulse (532 nm) from a Nd³⁺:YAG laser (Continuum, Surelite II) was used as an

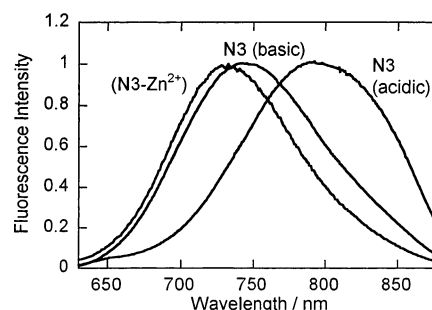


Figure 2. Emission spectra of synthesized (N3–Zn²⁺) and N3 in aqueous acidic (0.1 mol dm^{−3} HCl) and basic (0.1 mol dm^{−3} NaOH) solutions.

exciting light source. To measure microscopic fluorescence images, fluorescence collected with an objective lens (Mitsutoyo, 10x, NA = 0.28) was focused on the gated-CCD camera. Electron microscope images were recorded with a scanning electron microscope (SEM) (TOPCON, DS-720).

For the transient absorption measurements, a Xe flash lamp (Hamamatsu, L4642, 2 μ s pulse duration) was used as a probe light source. The probe light was focused on a sample specimen (2 mm in diameter). The area probed by the probe light was covered by that excited by the exciting light (10 mm in diameter). All measurements were carried out under the same optical geometry to obtain the relative yields of transient species. The probe light transmitted through the sample specimen was detected with a Si photodiode (Hamamatsu, S-1722) after being dispersed with a monochromator (Ritsu, MC-10N). Signals from the photodetector were processed with a digital oscilloscope (Tektronix, TDS680C) and were analyzed with a computer. All measurements were carried out at 295 K.

Results and Discussion

Formation of (N3–Zn²⁺) the Aggregate on the ZnO Surface Probed by Fluorescence Spectroscopy. Figure 2 shows the fluorescence spectra of N3 in basic (0.1 mol dm^{−3} NaOH) and acidic (0.1 mol dm^{−3} HCl) aqueous solutions. The fluorescence peaks are observed at 740 and 790 nm in basic and acidic solutions, respectively. The blue shift with increasing pH is due to the deprotonation of the carboxyl groups of N3,¹⁹ suggesting that the fluorescence peak position of N3 is sensitive to the type of an ion attached to carboxyl groups. Figure 2 also shows the fluorescence spectrum of a synthesized (N3–Zn²⁺) film. The peak observed at 730 nm is slightly blue-shifted from that of N3 in the basic solution (740 nm). This shift reflects the structure of the aggregate (N3–Zn²⁺), namely, N3 molecules are associated with each other through carboxyl groups by sharing Zn²⁺ ion. The fluorescence peak of (N3–Zn²⁺) can be distinguished from that of N3 in basic and acidic solutions. Therefore, the formation of (N3–Zn²⁺) on the surface of ZnO film can be probed by observing its fluorescence.

Figure 3 shows the absorption spectra of conc N3/ZnO and dil N3/ZnO films. The spectra are similar to each other, although the absorbance of the conc N3/ZnO film is 20 times as large as that of dil N3/ZnO. To identify the formation of (N3–Zn²⁺) on the surface of ZnO film, the fluorescence from N3/ZnO specimens was measured and is shown in Figure 3. For dil N3/ZnO, no emission can be observed with our apparatus. This indicates that the excited N3 is efficiently quenched by the electron injection to the ZnO films. On the contrary, fluorescence from conc N3/ZnO can be observed with a peak at 730 nm, which is identical to that of synthesized (N3–Zn²⁺) films. This clearly shows that (N3–Zn²⁺) is formed on conc N3/ZnO films.

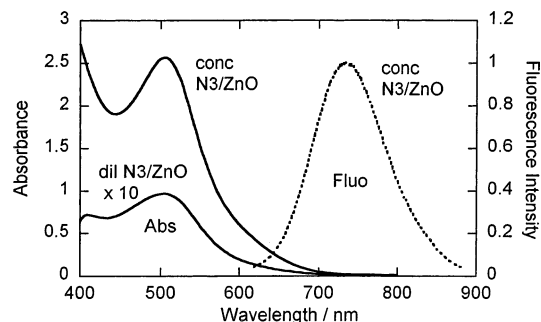


Figure 3. Absorption spectra of dil and conc N3/ZnO films and emission spectrum of conc N3/ZnO. The emission of dil N3/ZnO film cannot be observed.

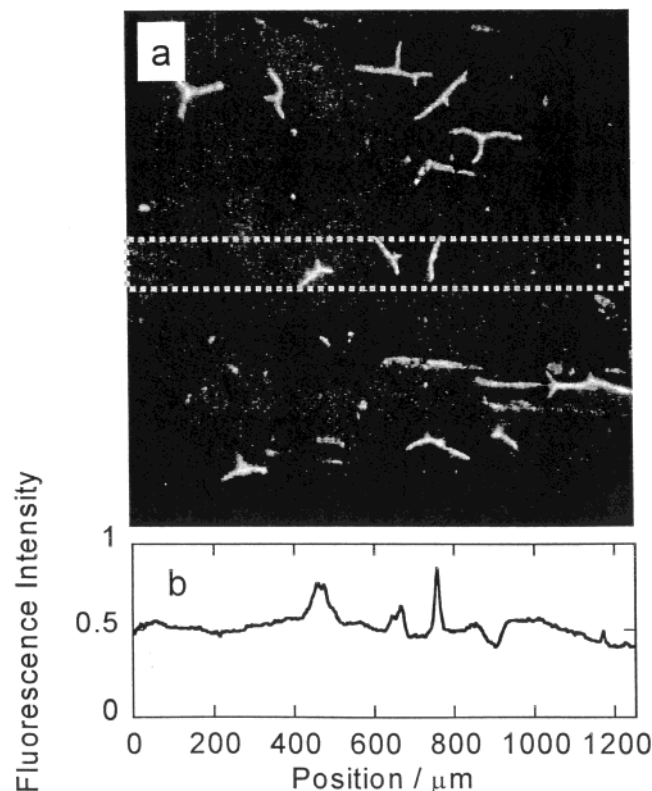


Figure 4. Fluorescence image of conc N3/ZnO (a). Intensity profile in the region indicated by dotted lines is also shown in part b.

Actually, we measured the sample specimens with various immersing times. When the sample specimens are immersed with long time (>3 h), we always observed the formation of the aggregates. However, the concentration of the aggregates is not always proportional to the immersing time, namely, the aggregation is very sensitive to the experimental condition. On the contrary, we found that the sample specimens without aggregates can be prepared with short immersing time (<10 min). Thus, we can study the excited-state properties of the aggregates and the effect of the aggregation on electron injection process.

Formation of Micrometer-Sized Particles of $(\text{N3}-\text{Zn}^{2+})$ on the ZnO Film Detected by Fluorescence and Scanning Electron Microscopy. As we mentioned above, the formation of $(\text{N3}-\text{Zn}^{2+})$ can be confirmed by observing its fluorescence. Accordingly, the microscopic image of the fluorescence directly shows the spatial distribution of $(\text{N3}-\text{Zn}^{2+})$ in the sample specimen. Figure 4a shows the fluorescence image of a conc N3/ZnO film. Many bright structures can be seen in the image. The bright structures in the image clearly show that micrometer-

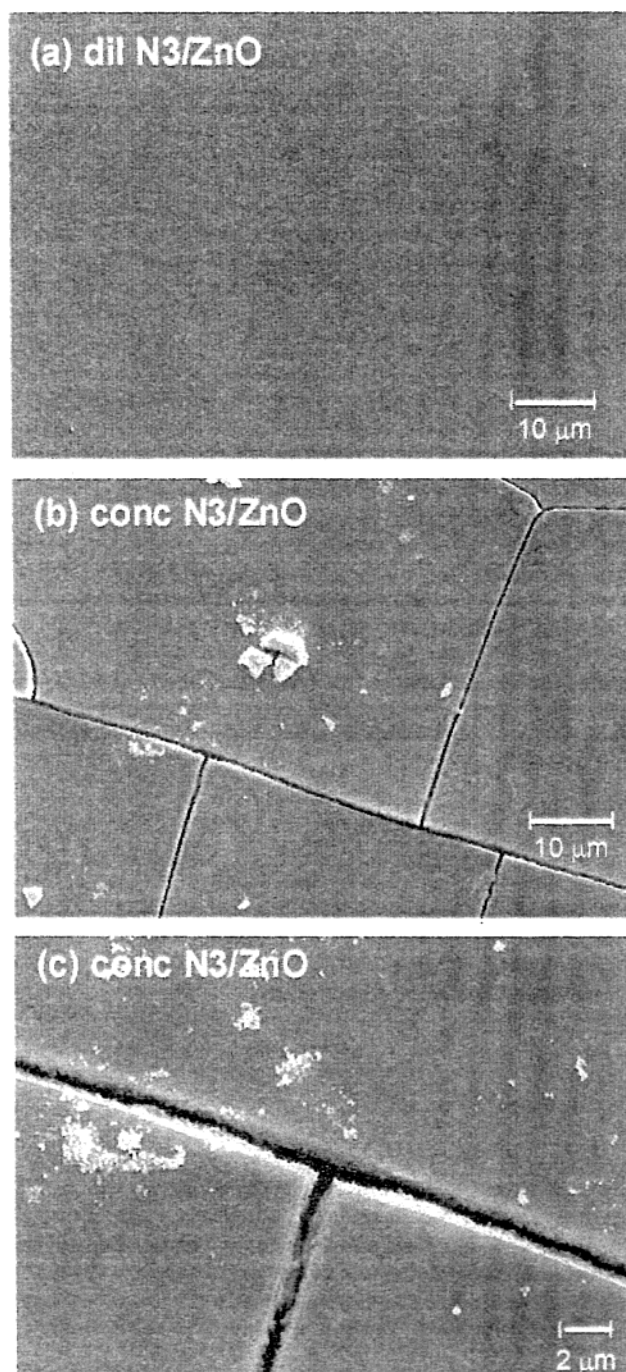


Figure 5. SEM images of dil N3/ZnO (a) and conc N3/ZnO (b) and that of conc N3/ZnO with higher spatial resolution (c).

sized crystals of $(\text{N3}-\text{Zn}^{2+})$ are formed in the sample specimen. Actually, the contrast of the image has been modified to obtain a clearer image, and the raw intensity profile of the fluorescence in the region indicated by dotted lines in the image is shown in Figure 4b. It shows that the fluorescence also comes from the dark area of the image, suggesting that aggregation also occurs in mesopores of the nanocrystalline films.

To observe the structure of the surface in detail, scanning electron microscopy (SEM) measurements were carried out. Figure 5a shows the SEM image of dil N3/ZnO, in which no $(\text{N3}-\text{Zn}^{2+})$ is formed. The surface of the film seems to be flat. With the present spatial resolution, mesoporous structures of the nanocrystalline ZnO film cannot be observed clearly. Figure 5b shows the SEM image of conc N3/ZnO with the same resolution as in Figure 5a. Many cracks of the substrate and

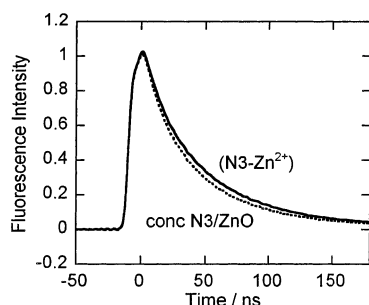


Figure 6. Fluorescence decay profiles of the synthesized (N3–Zn²⁺) and conc N3/ZnO films.

micrometer-sized crystals can be seen in the image. The sizes of the crystals are similar to those of (N3–Zn²⁺) observed as the bright structures in the fluorescence image, indicating that the micrometer-sized particles are attributable to (N3–Zn²⁺) on the surface of the ZnO film. Figure 5c shows the SEM image of conc N3/ZnO films with a higher resolution. Many small particles are observed along the cracks, suggesting that the cracks are formed by the stress induced by the crystal formation in the ZnO film. These cracks containing (N3–Zn²⁺) particles correspond to the bright lines observed in the fluorescence image.

Relative Electron Injection Efficiency Estimated by Transient Absorption Spectroscopy. The electron injection efficiency from excited (N3–Zn²⁺) to ZnO can be evaluated by observing its fluorescence lifetime. Figure 6 shows the fluorescence decays of a synthesized (N3–Zn²⁺) film and a (N3–Zn²⁺) on the conc N3/ZnO film. The excitation wavelength was 532 nm. The lifetime is found to be 42 ± 3 ns in the synthesized (N3–Zn²⁺) film and 38 ± 3 ns in (N3–Zn²⁺) on the conc N3/ZnO film. This clearly shows that at least part of excited (N3–Zn²⁺) do not inject electrons to ZnO in the conc N3/ZnO film. This can be explained from the results shown in Figures 4 and 5, namely, excited N3 dyes in (N3–Zn²⁺) are apart from the surface of the ZnO film by the formation of the micrometer-sized crystals.

The fluorescence lifetime measurement described above clearly shows that some of the aggregates do not inject electrons. However, for the conc N3/ZnO films, the monomers of N3 dye adsorbed on the surface may inject electrons to the ZnO films. In addition, the electron injection from the aggregates attached to the ZnO surface directly may also be possible. Thus, it is important to estimate the efficiency of the electron injection to compare it with the IPCE of N3/ZnO solar cells. We already reported that the relative efficiencies of electron injection can be obtained from the absorbance of oxidized sensitizer dyes observed by nanosecond transient absorption measurements, if all measurements are carried out under the same optical geometry and the correction of the number of absorbed photons are made precisely.²⁰

Figure 7a shows the transient absorption spectrum of the dil N3/ZnO film observed immediately after excitation (0 ns). The absorption band with a peak around 800 nm is observed, which can be assigned to oxidized N3.²¹ The oxidized form of N3 in dil N3/ZnO rises very fast and does not decay up to 200 ns (Figure 8). This indicates that the electron injection occurs immediately after excitation and the recombination is very slow, which is consistent with previous studies.²²

Figure 7b shows the transient absorption spectra of the conc N3/ZnO film observed at 0 ns and at 200 ns after excitation. As shown in Figure 8, the time profile of the absorption observed at 825 nm can be reproduced using two components,

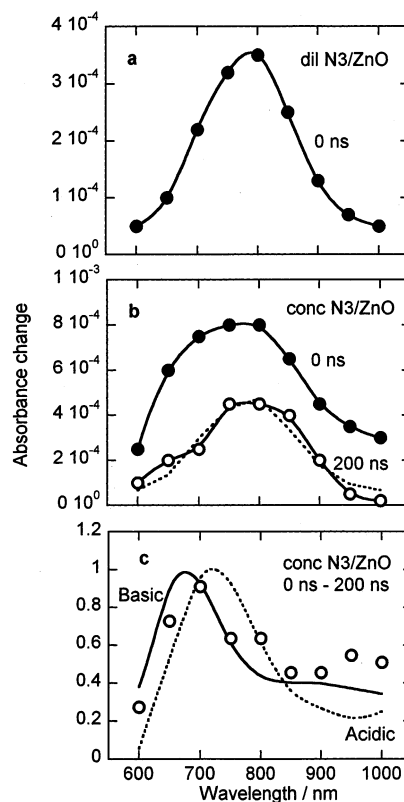


Figure 7. Transient absorption spectra of dil N3/ZnO recorded immediately (at 0 ns) after excitation (a) and at conc N3/ZnO at 0 ns (filled circles) and at 200 ns (open circles) (b). The dotted line in b is the spectrum of dil N3/ZnO at 0 ns normalized at 800 nm. The normalized spectrum of the fast component (0–200 ns) is also shown in c (open circles) together with those of acidic (dotted line) and basic (solid line) solutions of N3.

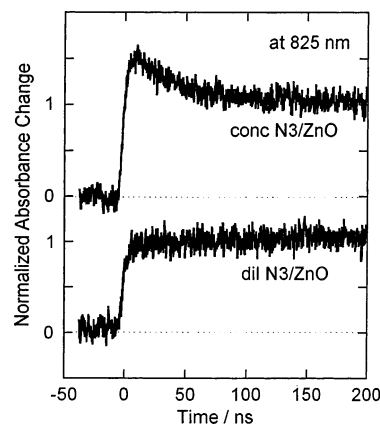


Figure 8. Time profiles of the transient absorption of dil N3/ZnO and conc N3/ZnO probed at 825 nm.

i.e., decay component with lifetime of $\tau_{\text{fast}} = 36 \pm 5$ ns and time-independent background. The fast decay species can be assigned to the excited (N3–Zn²⁺) from the similarity of the fluorescence lifetime of (N3–Zn²⁺) on conc N3/ZnO (38 ns). At 200 ns, the absorption due to excited (N3–Zn²⁺) decays completely and only the absorption band with the peak around 800 nm remains.

In Figure 7b, the spectrum of dil N3/ZnO at 0 ns normalized at 800 nm is also plotted by the dotted line. It is obvious that these spectra are similar to each other. As shown in Figures 2 and 7c, the spectra of fluorescence and transient absorption of (N3–Zn²⁺) are different from those of the monomeric form of N3, suggesting that the electronic state of N3 is perturbed by

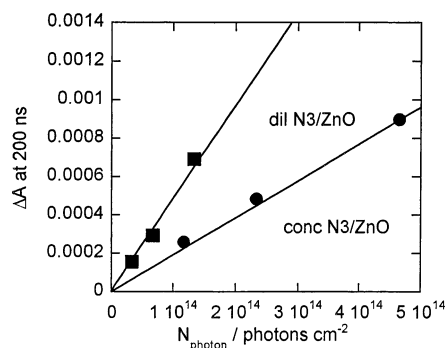


Figure 9. Absorbance changes at 200 ns after the excitation, probed at 825 nm, as a function of the number of absorbed photons for dil N3/ZnO and conc N3/ZnO. The slope of the straight line gives the relative efficiency of electron injection from excited sensitizer dyes to ZnO films.

the aggregation. Accordingly, the 200 ns spectrum of conc N3/ZnO can be assigned to the oxidized form of the monomeric N3, namely, the electron transfer mainly occurs from excited monomeric N3. This implies that the aggregates are formed on the surface covered with the monomeric N3.

The spectrum of the fast decay component in Figure 7b can be obtained by subtracting the spectrum at 200 ns from that at 0 ns (Figure 7c). It is obvious that the spectrum of the fast component is different from that of the oxidized N3 dye, suggesting that the fast decay is not due to charge recombination. In the figure, the transient absorption spectra of N3 in acidic and basic solutions are also shown for comparison. The spectrum of the fast component is slightly different from those of N3 in acidic and basic solutions. This indicates that the transient absorption spectrum of N3 is sensitive to the ions attached to the carboxyl groups.

The relative injection efficiency $\Phi_{\text{inj}}^{\text{rel}}$ can be expressed as follows by using the absorbance change A_{ox} of the oxidized N3 dye and the number N_{photon} of absorbed photons:

$$\Phi_{\text{inj}}^{\text{rel}} = \frac{A_{\text{ox}}}{N_{\text{photon}}} \quad (1)$$

From A_{ox} , it is possible to estimate the absolute value of the number of oxidized N3 dye, if the molar absorption coefficient is available. At present, the coefficient is not known, so we cannot estimate the absolute value of Φ_{inj} .

In both samples, the electron injection occurs mainly from monomeric form of N3, as we discussed above. Thus, the relative efficiency of the electron injection can be evaluated from the absorbance because of the oxidized form of N3. For conc N3/ZnO, the absorptions of the excited (N3-Zn^{2+}) and of the oxidized N3 dye overlap with each other. As shown in Figure 8, the absorption of the excited (N3-Zn^{2+}) decays completely at 200 ns and that of the oxidized N3 dye does not. Therefore, the relative efficiency can be evaluated from the absorbance change at 200 ns.

Figure 9 shows A_{ox} at 825 nm as a function of the number N_{photon} of absorbed photons evaluated as a product of the exciting light intensity I_{ex} and the light harvesting efficiency, $1 - T$, where T is the transmittance of the sample specimen at the excitation wavelength (532 nm). It has been pointed out that the decay becomes faster with increasing excitation intensity.²³ Thus, we measured the transient absorption under weak excitation conditions ($I_{\text{ex}} = 0.04\text{--}0.14 \text{ mJ cm}^{-2}$). Under this condition,

the decay profile is not sensitive to the exciting light intensity. As seen from Figure 9, A_{ox} is proportional to N_{photon} , and the slope of the line gives the relative efficiency of the electron injection (see eq 1). The electron injection efficiency is decreased by the aggregation, namely, the electron injection efficiency of conc N3/ZnO is about one-third of that of dil N3/ZnO. For dil N3/ZnO, no emission and no absorption due to the excited state are observed, suggesting that the electron injection efficiency Φ_{inj} of dil N3/ZnO is almost unity. Under this assumption, Φ_{inj} of conc N3/ZnO can be estimated to be about 0.3.

Conclusion

We have found that the aggregation of N3 dyes with Zn^{2+} ions proceeds during the preparation of the dye-sensitized films. The aggregates are produced in mesopores of the nanocrystalline film. In addition, the micrometer-sized crystals of the aggregates are formed on the surface of the film. The electron injection from the aggregate does not occur efficiently, and therefore, the overall electron injection efficiency of the sample specimen is decreased by the aggregation. It should be emphasized that the nanocrystalline ZnO film is a promising material for high performance solar cells, if the formation of aggregates between sensitizer molecules and Zn^{2+} ions can be effectively prevented.

Acknowledgment. This work was supported by COE development program of MEXT of Japan.

References and Notes

- (1) Nazeruddin, M. K.; Kay, A.; Rodicio, I.; Humphry-Baker, R.; Müller, E.; Liska, P.; Vlachopoulos, N.; Grätzel, M. *J. Am. Chem. Soc.* **1993**, *115*, 6382–6390.
- (2) Hagfeldt, A.; Grätzel, M. *Acc. Chem. Res.* **2000**, *33*, 269–277.
- (3) Jelly, E. E. *Nature* **1936**, *138*, 1009–1010.
- (4) Kobayashi, T. *J-Aggregates*; World Scientific: Singapore, 1996.
- (5) Rubtsov, I. V.; Ebina, K.; Satou, F.; Oh, J.-W.; Kumazaki, S.; Suzumoto, T.; Tani, T.; Yoshihara, K. *J. Phys. Chem. A* **2002**, *106*, 2795–2802.
- (6) Tani, T. *Photographic Sensitivity*; Oxford University Press: Oxford, 1995.
- (7) Aguirresacona, I. L.; Arbeloa, F. L.; Arbeloa, I. L. *J. Chem. Educ.* **1989**, *66*, 866–869.
- (8) Nasr, C.; Liu, D.; Hotchandani, S.; Kamat, P. V. *J. Phys. Chem.* **1996**, *100*, 11054–11061.
- (9) Horiuchi, H.; Katoh, R.; Murata, S.; Tachiya, M. to be published.
- (10) Kay, A.; Grätzel, M. *J. Phys. Chem.* **1993**, *97*, 6272–6277.
- (11) Khazraji, A. C.; Hotchandani, S.; Das, S.; Kamat, P. V. *J. Phys. Chem. B* **1999**, *103*, 4693–4700.
- (12) Sayama, K.; Tsukagoshi, S.; Hara, K.; Ohga, Y.; Shinpou, A.; Abe, Y.; Suga, S.; Arakawa, H. *J. Phys. Chem. B* **2002**, *106*, 1363–1371.
- (13) Redmond, G.; Fitzmaurice, D.; Grätzel, M. *Chem. Mater.* **1994**, *6*, 686–691.
- (14) Resmo, H.; Keis, K.; Lindström, H.; Södergren, S.; Solbrand, A.; Hagfeldt, A.; Lindquist, S.-E. *J. Phys. Chem. B* **1997**, *101*, 2598–2601.
- (15) Bedja, I.; Kamat, P. V.; Hua, X.; Lappin, A. G.; Hotchandani, S. *Langmuir*, **1997**, *13*, 2398–2403.
- (16) Baumeler, R.; Rys, P.; Zollinger, H. *Helv. Chim. Acta* **1973**, *56*, 24502460.
- (17) Hauffe, K. H. *Photogr. Sci. Eng.* **1976**, *20*, 124.
- (18) Keis, K.; Lindgren, J.; Lindquist, S. E.; Hagfeldt, A. *Langmuir* **2000**, *16*, 4688–4694.
- (19) Nazeeruddin, M. K.; Zakeeruddin, S. M.; Humphry-Baker, R.; Jirousek, M.; Liska, P.; Vlachopoulos, N.; Shklover, V.; Fisher, C. H.; Grätzel, M. *Inorg. Chem.* **1999**, *38*, 6298–6305.
- (20) Hara, K.; Horiuchi, H.; Katoh, R.; Singh, L. P.; Sugihara, H.; Sayama, K.; Murata, S.; Tachiya, M.; Arakawa, H. *J. Phys. Chem. B* **2002**, *106*, 374–379.
- (21) Tachibana, Y.; Moser, J. E.; Grätzel, M.; Klug, D. R.; Durrant, J. R. *J. Phys. Chem.* **1996**, *100*, 20056–20062.
- (22) Willis, R. L.; Olson, C.; O'Regan, B.; Lutz, T.; Nelson, J.; Durrant, J. R. *J. Phys. Chem. B* **2002**, *106*, 7605–7613.
- (23) Haque, S. A.; Tachibana, Y.; Willis, R. L.; Moser, J. E.; Grätzel, M.; Klug, D. R.; Durrant, J. R. *J. Phys. Chem. B* **2000**, *104*, 538–547.